Catalysis Today 175 (2011) 494–503

Contents lists available at ScienceDirect

Catalysis Today

journal homepage: www.elsevier.com/locate/cattod

Anti-ASF distribution in Fischer-Tropsch synthesis over unsupported cobalt catalysts in a batch slurry phase reactor

Xiaohao Liu[a,b], Akiyuki Hamasaki[a,b], Tetsuo Honma[c], Makoto Tokunaga[a,b,*]

[a] Department of Chemistry, Graduate School of Science, Kyushu University, Higashi-Ku, Fukuoka 812-8581, Japan
[b] JST (Japan Science and Technology Corporation), CREST, Japan
[c] Japan Synchrotron Radiation Research Institute (JASRI), Japan

ARTICLE INFO

Article history:
Received 1 October 2010
Received in revised form 3 February 2011
Accepted 14 March 2011
Available online 8 April 2011

Keywords:
Fischer-Tropsch Synthesis
Cobalt catalysts
Water addition
Anti-ASF distribution
Selective synthesis

ABSTRACT

Fischer-Tropsch synthesis (FTS) over unsupported coprecipitated cobalt catalysts in *n*-decane in a batch slurry phase reactor by adding water vapor ($H_2O/CO = 0.12$ in molar ratio) prior to reaction has been studied. The addition of water vapor exhibits a marked effect on the product selectivity. In the absence of water, the carbon number distribution of FT products follows the classical Anderson-Schulz-Flory (ASF) pattern resulting in a low selectivity (32%) in the desired C_{10+} hydrocarbons. In contrast, with the promotion of water vapor, the formation of heavy products is appreciably increased up to 87.3% in C_{10+} hydrocarbons so that the selectivity in the range of C_8–C_{30} increases obviously along with an increase in carbon number (n), which leads to a substantial deviation from ASF pattern. The effect of water is explained by suppressing secondary hydrogenation of 1-olefins and facilitating their readsorption and chain growth.

1. Introduction

As petroleum reserves dwindle and stringent environmental regulations have been enacted, the world will increasingly rely on Fischer-Tropsch synthesis (FTS) which is a reductive oligomerization process of synthesis gas (syngas) consisting of CO and H_2 to produce super clean fuels and chemicals from the vast reserves of coal, natural gas, oil shale, and tar sands, or from biomass [1]. Since the products produced by FTS are a wide range of hydrocarbon from C_1 to > C_{100} not selective for any specific desired fraction owing to its essence of polymerization, controlling the selectivity to desired product is of great importance.

FTS mainly produces normal (*n*-) hydrocarbons (*n*-paraffins and 1-olefins) as the primary products, and the *n*-hydrocarbons in the range of C_5–C_{10} have poor octane number rating not favorable for its direct use for gasoline engines [2–6]. Methane in the highest selectivity and ethane are needed to be reformed into syngas, in addition, the recycling between methane and syngas decreases the process efficiency. In contrast, *n*-hydrocarbons in the range of ~C_{11}–C_{20} with high cetane number rating constitute an ideal fuel for diesel engines which runs ~30% more efficiently than gasoline engines [7,8]. The wax (C_{21+}) produced by FTS has been recognized as high qualities and stabilities and which is aromatics- and sulfur-free [9,10].

Normally, FT product distribution follows Anderson-Schulz-Flory (ASF) pattern, in such cases the logarithm mole of the product ($\log W_n/n$, W_n is the mass fraction of a particular product) is linearly plotted against carbon number (n) [11–14], which brings a persistent interest in selective synthesis of products [15]. Probability of chain growth (α value) is the ratio of the chain propagation rate constant to the chain propagation plus the chain termination rate constants. The chain growth factor (α) is determined by catalyst structure and composition, reaction phase (gas-, liquid-, gas–liquid-, and supercritical- phase), and reaction parameter, such as temperature, syngas partial pressure, H_2/CO ratio in feed gas. Although the high chain growth factor (α) can increase the selectivity in heavy products, the ASF pattern always leads to a gradual decrease in selectivity with an increase in carbon number (n), which limits the formation of desired middle distillates and heavy hydrocarbons (wax) [11–14,16]. Therefore, it is preferable to produce higher hydrocarbons in anti-ASF manner to obtain suitable heavy products.

It is believed that the readsorption and subsequent secondary reactions (hydrogenolysis, cracking, and reinsertion) of the primary 1-olefin products are the main reasons for the deviation from ASF distribution and several researchers have reported the deviations from ASF pattern in FTS [17–19]. However, these deviations are not noticeable mainly because secondary hydrogenation is the main

* Corresponding author at: Kyushu University, Department of Chemistry, 6-10-1 Hakozaki, Higashi-ku, Fukuoka, 812-8581, Japan. Tel.: +81 92 642 7528; fax: +81 92 642 7528.
E-mail address: mtok@chem.kyushu-univ.jp (M. Tokunaga).

0920-5861/$ – see front matter © 2011 Elsevier B.V. All rights reserved.
doi:10.1016/j.cattod.2011.03.030

reaction pathway and the light 1-olefins are relatively more difficult to be readsorbed onto the catalytic sites for secondary reactions due to chain length dependent diffusion limitation [20–23], solubility [24–27], and physisorption. One of the present authors has confirmed in a previous report that secondary hydrogenation of primary 1-olefins is the main reaction pathway, which resulted in no deviation from ASF pattern while the selectivity of 1-olefin is greatly changed by selecting solvent [28–30]. The author has also demonstrated that 1-olefin addition (1-olefin/CO = 0.16 in molar ratio) to FTS in a three-phase fixed-bed reaction system can achieve anti-ASF pattern to a larger extent [31,32]. Heavy hydrocarbons are thus increased remarkably while suppressing the formation of light hydrocarbons, which is attributed to chain growth from the added 1-olefin by CH_2 incorporation. However, 1-olefins as chemicals are very valuable. It is not economical to shift the carbon number distribution towards the desired fraction through the adding 1-olefins. In this paper, we report a remarkable deviation from ASF distribution arises from the effect of added water which suppresses the secondary hydrogenation.

In the FTS over Co-based catalysts, oxygen atoms in CO are mainly removed as water. The cobalt catalysts do not exhibit significant water gas shift (WGS) activity and thus the water partial pressure increases with increasing CO conversion and residence time. Therefore, studies on the effects of water in FTS are quite important. The effects of water on the performance of the Co catalysts are examined in both fixed-bed and slurry phase reactors by several researchers [33–39], which are described to be either negligible [40–42], or negative [34,43], or positive [33,44]. The negative is concerned to the formation of inactive cobalt oxides or irreducible cobalt-support compounds. As for positive effects, water may affect syngas conversion and product selectivity such as higher catalytic activity and higher chain growth factor (α). However, any remarkable anti-ASF pattern has not appeared in literature, which might be due mainly to inefficient utilization of light primary 1-olefins whose low boiling points result in a short residence time in a flow-type fixed bed or in a slurry phase reactor [45].

Recently, we reported that coprecipitated Au/Co_3O_4 catalysts are effective for the heterogeneous hydroformylation of olefins [46]. The selectivity above 85% is the desired aldehydes and the Au/Co_3O_4 catalyst can be recycled at least 4 times by simple decantation. The gold nanoparticles act as a source of spillover H reducing Co_3O_4 at a temperature about 200 °C lower than the reduction of pure Co_3O_4 (350–400 °C). The reduced Co metal catalyzes the hydroformylation reaction.

In the present work, we try to utilize unsupported Au/Co_3O_4 as a FTS catalyst in the presence of water. The gold as a reduction promoter may inhibit the oxidation of Co metal by water. As reported by Nowitzki et al. [47], an alumina-supported palladium shell around the cobalt for FTS can prevent Co oxidation in H_2O/H_2. Thus, an unsupported Co_3O_4 was selected for our study on the effects of water for avoiding some additional effects on water sensitive support and the formation of irreducible cobalt-support compounds. This study is to markedly increase the selectivity of middle distillates and/or heavy wax by adding water. The amount of added water ($H_2O/CO = 0.12$ in molar ratio) is much less than that ($H_2O/CO = 0.6$ in molar ratio) did not deactivate unsupported Co_3O_4 in a continuous stirred tank reactor (CSTR) [48]. Water is expected to affect the chain growth and secondary reaction pathway (depressing the hydrogenation and promoting the chain growth) for *in situ* formed 1-olefins. The 1-olefins not added but *in situ* formed are efficiently utilized, which leads to anti-ASF patterns. Thus, the selectivity of wax is remarkably increased to realize a highly economical process. A batch slurry phase reactor is selected for the study based on the consideration that all *in situ* formed 1-olefins can be repeatedly used for secondary chain growth before they are terminated as *n*-alkanes.

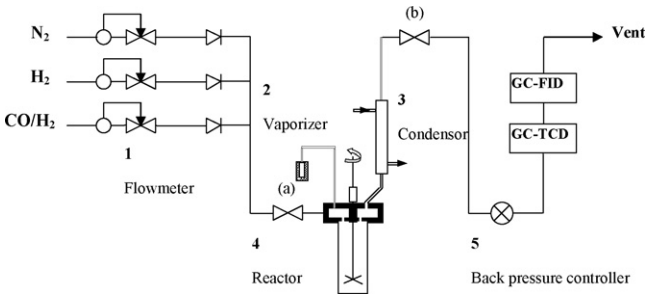

Fig. 1. Schematic flow diagram of slurry phase FTS apparatuses.

2. Experimental

2.1. Preparation of catalysts

The Au/Co_3O_4 catalysts were prepared by coprecipitation method. This was performed by adding aqueous solution of cobalt (II) nitrate hexahydrate and $HAuCl_4$ to sodium carbonate aqueous solution at one time at room temperature. The coprecipitates were washed with distilled water to remove as much of the sodium and chloride as possible. The wet solids were dried at 100 °C overnight and then calcined in air at 400 °C for 4 h. The Co_3O_4 was prepared in the same procedure. The gold loading was expressed by atom% = 100 × Au/(Au + M).

2.2. Catalyst characterization

Powder X-ray diffraction (XRD) studies were carried out with a RINT 2000 system (Rigaku) diffraction meter using Cu-K_α radiation. The Brunauer-Emmett-Teller (BET) surface areas and pore volumes were determined from nitrogen adsorption and desorption isotherm data obtained at 77.3 K using an Autosorb-1 apparatus (Quantachrome). The microstructures of calcined samples were studied by transmission electron microscope (TEM) images obtained on a JEM 2100XS instrument (JEOL) operated at 200 kV. The Co K edge XAFS measurements were made on BL14B2 beam line at Spring-8, Sayo-cho, Hyogo, Japan.

2.3. Catalytic reactions for FTS

A batch slurry phase reactor is best suited to study the effects of water on product selectivity. Fig. 1 shows a flow diagram of the experimental unit. First, catalyst (150 mg) and solvent *n*-decane (14.6 g) were added into reactor in sequence. The reactor was purged by hydrogen twice and then vaporize water in 2 into reactor as shown in Fig. 1. The inlet (a) and outlet (b) of the reactor were closed and open the condenser 3. The vaporized water (10 mmol) was then condensed into water liquid uniformly on the wall of reactor and condenser. The pressure was increased to a given initial pressure (6 MPa) at room temperature by a 20 ml/min syngas ($Ar/CO/H_2 = 3/32.3/64.7$) flow. CO added is 84.1 mmol ($H_2O/CO = 0.12$ in molar ratio). The mixture was then stirred mechanically (1000 r/min) and the temperature was elevated to reaction temperature (230 °C). After reaction, the mixture was cooled to room temperature and the gas-phase mixture was analyzed by a thermal conductivity detector (TCD) coupled with a flame ionisation detector (FID) to determine CO conversion and C_1–C_5 hydrocarbon content. Liquid-phase product was analyzed using a GC 6850 (Agilent) equipped with HP–1 Column (J&W, length 30 m, 0.32 mm I.D.) for C_3–C_{40} hydrocarbons. Hydrocarbon selectivity (%) is calculated by weight base.

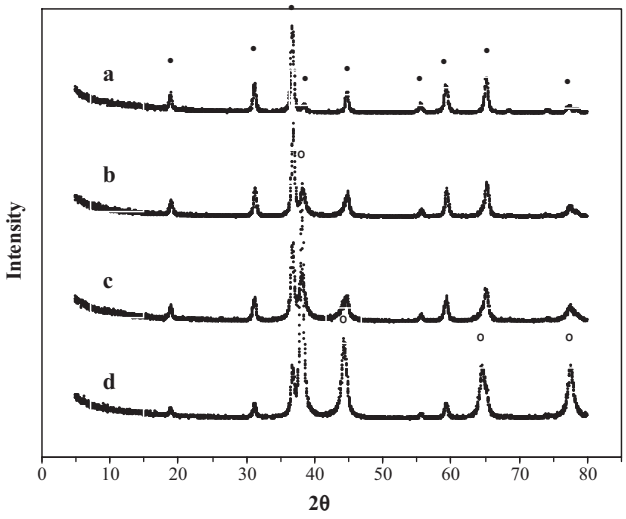

Fig. 2. X-ray diffraction patterns of Co_3O_4 and Au/Co_3O_4 catalysts prepared by coprecipitation. (a) Co_3O_4; (b) 5 atom% Au/Co_3O_4; (c) 10 atom% Au/Co_3O_4; (d) 25 atom% Au/Co_3O_4. (●) Co_3O_4; (○) Au.

3. Results

3.1. Catalyst characterization

3.1.1. X-ray diffraction

Fig. 2 shows XRD patterns of Co_3O_4 and Au/Co_3O_4 (5 atom%, 10 atom%, and 25 atom% gold loading) catalysts. The diffraction peaks at $2\theta = 19.0^\circ$, 31.4°, 36.9°, 38.6°, 44.7°, 55.7°, 59.3°, 65.2°, 74.1°, 77.5° are those of Co_3O_4. The peaks of Au are at $2\theta = 38.2^\circ$, 44.4°, 64.7°, 77.6°. It is evident that the peaks belonging to Au become stronger along with an increase in gold loading from 0 to 25 atom% as shown in Fig. 2a–d [28,49,50].

3.1.2. Structural properties

As shown in Table 1, the specific surface area and pore structure of catalysts were markedly affected by gold loading. The specific surface area decreases with an increase in gold loading and is the smallest for 25 atom% Au/Co_3O_4, whereas the pore volume and pore diameter reach maxima at 5 or 10 atom% gold loading and are almost similar to each other for Co_3O_4 and 25 atom% Au/Co_3O_4 but much lower than those of 5 or 10 atom% gold loading.

3.1.3. TEM images

TEM images of the Au/Co_3O_4 catalysts prepared by coprecipitation followed by calcination at 400 °C are shown in [46]. Irrespective of different gold loadings, Co_3O_4 particles are similar in size at around 20–40 nm, while the size of Au particles changes with gold loadings. Five atom% gold loading leads to a low population of Au nanoparticles with sizes of 3–10 nm on the surfaces of Co_3O_4. The change in the size of Au nanoparticles for 10 atom% Au/Co_3O_4 is not obvious. However, the percentage of larger gold particles (6–10 nm) and the population of gold particles on Co_3O_4 increase. In the case of 25 atom% Au/Co_3O_4, the TEM image indicates that the Au seems to give rise to coating-like patterns on Co_3O_4 and may not form clear nanoparticles.

Table 1
Physicochemical properties of Au/Co_3O_4 catalysts with different Au loadings prepared by co-precipitation followed by calcinations at 400 °C.

Catalyst	Specific surface area ($m^2\ g^{-1}$)	Total pore volume ($cm^3\ g^{-1}$)	Average pore diameter (nm)
Co_3O_4	45.5	0.03	2.2
5 atom% Au/Co_3O_4	43.1	0.22	20.5
10 atom% Au/Co_3O_4	40.1	0.19	19.3
25 atom% Au/Co_3O_4	17.8	0.01	2.2

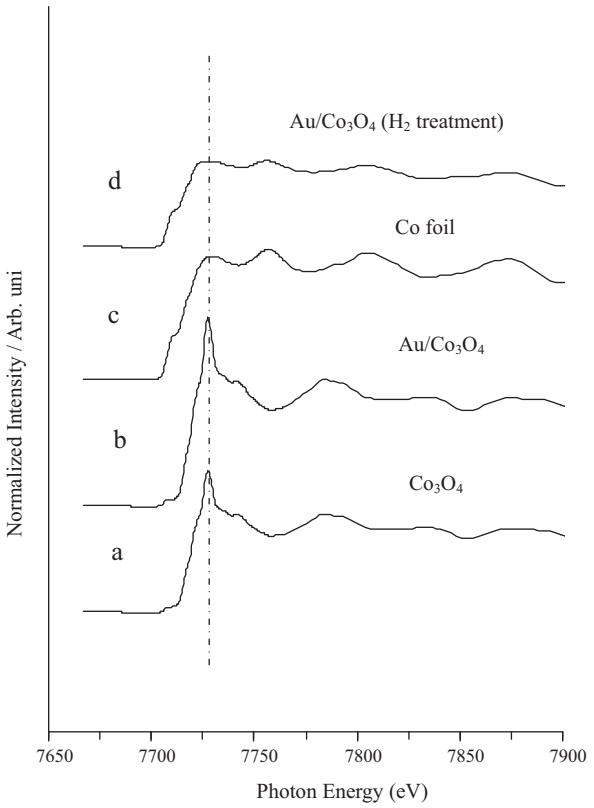

Fig. 3. Normalized Co K edge XANES spectra for cobalt compounds (a) reference Co_3O_4, (b) 5 atom% Au/Co_3O_4 prepared by co-precipitation, (c) reference Co foil, and (d) 5 atom% Au/Co_3O_4 by reduction pretreatment (2.0 MPa, 100 °C, 3 h) in *n*-heptane.

3.1.4. XANES spectra

The XANES spectra for the cobalt reference compounds (a) Co_3O_4 and (c) Co foil and (b) calcined 5 atom% Au/Co_3O_4 and (d) 5 atom% Au/Co_3O_4 by H_2 treatment (2 MPa, 100 °C, 3 h) in *n*-heptane is shown in Fig. 3. It is clear that the calcined 5 atom% Au/Co_3O_4 prior to reduction is very similar to reference Co_3O_4 (Fig. 3a and b). After reduction, a strong absorption with unique spectral feature (ca. 7725 eV) disappeared. The reduced 5 atom% Au/Co_3O_4 closely resembles the spectrum of a Co foil (Fig. 3c and d), which shows that Co_3O_4 is fully reduced Co metal by H_2 treatment [51].

3.2. Catalytic results

3.2.1. Addition of water in vapor and liquid

Table 2 and Fig. 4 show the catalytic results in FTS by addition of water. In the absence of water addition, the product selectivity gives a rapid decrease with an increase in carbon number (*n*) (Fig. 4A), which obeys the ASF pattern, although the reaction itself produces a large amount of water (47.3 mmol at 71% convn). Total selectivity for desired C_{21}–C_{40} hydrocarbons is as low as 6.5% (Table 2, entry 1). By aid of water vapor (10 mmol, $H_2O/CO = 0.12$ in molar ratio) that is far smaller than that of the FT water product, a novel carbon number distribution substantially deviated from the conventional ASF pattern, which resulted in a hydrocarbon selectivity increasing with an increase in carbon number ($n = 7$–27) (Fig. 4B). In this case, the selectivity in desired C_{10}–C_{20} and C_{21}–C_{40} reached 27.9% and

Table 2
Effect of water addition on the product selectivity of FTS.

Entry	Addition of water	$P_{after\ reaction}$ (MPa)	CO conversion (%)	Selectivity (%)					
				C_1	C_2	C_{3-4}	C_{5-9}	C_{10-20}	C_{21-40}
1	No	2.0	71.0	11.2	8.7	20.1	28.1	25.5	6.5
2	Water vapor	1.7	74.2	3.9	0.9	4.1	9.0	27.9	59.4
4	Water liquid	1.8	68.2	5.0	1.2	6.6	10.3	24.7	42.5

Reaction conditions: 5 atom% Au/Co_3O_4 catalyst = 150 mg; T = 230 °C; $P_{initial\ synthesis\ gas}$ = 6 MPa (Ar/CO/H_2 = 3/32.3/64.7); reaction time = 11 h; solvent *n*-decane = 14.6 g; water vapor added = 10 mmol; the reactions were carried out in a closed autoclave reactor.

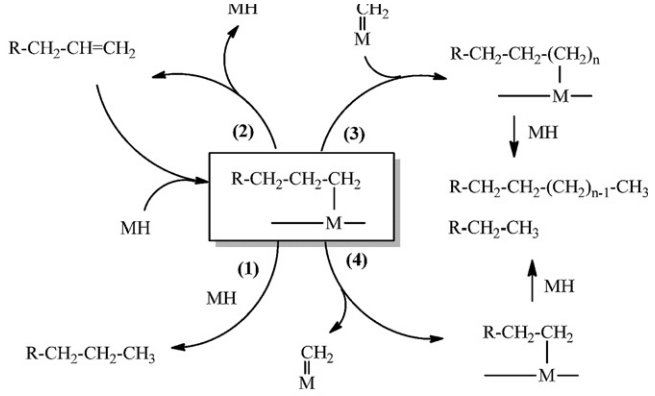

in which M indicates a surface adsorption site

Scheme 1. Secondary reactions of *in situ* formed 1-olefins over Au/Co_3O_4 catalyst.

59.4% (Table 2, entry 2), respectively. As shown in Fig. 4C, a similar carbon number distribution is obtained by the addition of liquid in the same amount as water vapor. By comparison of these results, the addition of water vapor affects more positive in the synthesis of the heavy hydrocarbons rather than water liquid.

3.2.2. Effect of time on stream on product selectivity

As shown in Table 3 and Fig. 5, addition of water vapor in FTS over unsupported Co_3O_4 catalysts caused a strong effect on product selectivity and ASF pattern with time on stream (TOS). The product selectivity in the range of C_{21}–C_{40} remarkably increased from 32.7% to 59.4% with a corresponding decrease in light hydrocarbons (C_1–C_9) from 44.8% to 23.1% (Table 3, entries 1 and 2). The carbon number distribution rapidly deviated from the conventional ASF pattern to a larger extent when the reaction time extended from 11 h to 23 h (Fig. 5A and B). Interestingly, at a longer reaction time (42 h), the carbon number distribution followed the conventional ASF pattern leading to a low selectivity (29.5%) in C_{21}–C_{40} (Table 3, entry 4; Fig. 5B), although small change of CO conversion was observed (74.2–81.9%).

3.2.3. Effect of temperature on product selectivity

The effect of temperature on the product selectivity and the carbon number distribution by addition of water vapor is presented in Table 4 and Fig. 6. The anti-ASF patterns appeared at both 230 °C and 250 °C (Fig. 6B). At 230 °C, selectivity of the desired heavy hydrocarbons C_{21}–C_{40} (Table 4, entry 2, 54.7%) was about 3 times of that at 250 °C (Table 3, 17.1%). When the reaction was operated at a lower temperature 215 °C, selectivity of the hydrocarbons in C_{21}–C_{40} (Table 4, entry 1, 40.8%) was decreased. Fig. 6A shows clearly the selectivity for hydrocarbons C_{25}–C_{38} (230 °C case) was much higher than that of the lower hydrocarbons (C_7–C_{24}). Consequently, optimal reaction temperature could maximize the selectivity in desired hydrocarbons.

3.2.4. Effect of gold loading in Au/Co_3O_4 on product selectivity

The gold loading obviously affected the product selectivity in FTS over Au/Co_3O_4 catalysts in the presence of water as shown in Table 5 and Fig. 7. A high gold loading (10 or 25 atom%) led to a similar carbon number distribution (Fig. 7A) to that at 250 °C (Fig. 6A). Compared to pure Co_3O_4, the selectivity in C_1–C_9 for 10 atom% Au/Co_3O_4 was notably increased from 32% (Table 5, entry 1) to 69.2% (Table 5, entry 3). Correspondingly, the selectivity in C_{21}–C_{40} was decreased from 54.2% (Table 4, entry 1) to 22.7% (Table 4, entry 3). A low gold loading (5 atom%) did not change the product selectivity compared to that of pure Co_3O_4 (Table 5, entries 1 and 2).

3.2.5. Hydrogenolysis of FT products and n-dotriacontane (n-$C_{32}H_{66}$)

As mentioned above, a long reaction time (42 h) resulted in a conventional ASF pattern and low selectivities in heavy hydrocarbons (Table 3, entries 3 and 4). It is supposed that the formed heavy hydrocarbons (C_{21}–C_{40}) have been hydrogenolyzed into lower hydrocarbons due to low syngas pressure at late stage. To confirm this hypothesis, the hydrogenolysis of FT products obtained at 23 h (TOS) was carried out in the absence of water at 230 °C and 3 MPa H_2 for 30 h. A quite interesting phenomenon appeared such as the carbon number distribution changed from anti-ASF pattern to linear ASF pattern (Fig. 8B).

Table 3
Effect of time on stream (TOS) on the product selectivity of FTS over coprecipitated Co_3O_4.

Entry	Time on stream (h)	$P_{after\ reaction}$ (MPa)	CO conversion (%)	Selectivity (%)					
				C_1	C_2	C_{3-4}	C_{5-9}	C_{10-20}	C_{21-40}
1	6	4.9	19.9	3.4	1.1	10.6	29.4	19.9	35.7
2	11	4.1	33.2	4.4	1.9	11.1	27.4	22.5	32.7
3	23	1.7	74.2	3.9	0.9	4.1	14.2	17.5	59.4
4	42	1.3	81.9	6.9	4.2	10	29.2	20.1	29.5

Reaction conditions: Co_3O_4 = 150 mg; T = 230 °C; $P_{initial\ synthesis\ gas}$ = 6 MPa (Ar/CO/H_2 = 3/32.3/64.7); solvent *n*-decane = 14.6 g; water vapor added = 10 mmol; the reactions were carried out in a closed autoclave reactor.

Table 4
Effect of reaction temperature on the product selectivity of FTS over the coprecipitated 5 atom% Au/Co_3O_4.

Entry	Temperature (°C)	$P_{after\ reaction}$ (MPa)	CO conversion (%)	Selectivity (%)					
				C_1	C_2	C_{3-4}	C_{5-9}	C_{10-20}	C_{21-40}
1	215	1.6	77.0	4.6	1.6	10.2	29.2	13.7	40.8
2	230	1.7	74.5	5.6	1.4	5.7	19.1	13.5	54.7
3	250	1.9	71.7	15.7	8.9	19.2	28.9	10.1	17.1

Reaction conditions: 5 atom% Au/Co_3O_4 = 150 mg; $P_{initial\ synthesis\ gas}$ = 6 MPa ($Ar/CO/H_2$ = 3/32.3/64.7); reaction time = 11 h; solvent *n*-decane = 14.6 g; water vapor added = 10 mmol; the reactions were carried out in a closed autoclave reactor.

In order to reveal the hydrogenolysis hypothesis of *n*-hydrocarbons, a model compound *n*-dotriacontane (*n*-$C_{32}H_{66}$) was selected for study. Fig. 9 showed that high temperature and/or low H_2 partial pressure promoted its successive hydrogenolysis to give a wide range of *n*-hydrocarbon whose selectivity is decreased with a decrease in carbon number (*n*). It was also found that plots of $\log W_n/n$ against the carbon number (*n*) brought straight lines over hydrogenolyzed products, which suggests that *n*-alkane hydrogenolysis is a reverse process of its formation in FTS by monomer CH_2 polymerization.

4. Discussion

Syngas (CO and H_2) is converted to hydrocarbons via FTS over a heterogeneous catalyst containing a group VIII metal (Fe, Co, Ru). CO and H_2 are at first dissociated on the catalyst surface and converted into CH_x species and H_2O [52]. The alkyl chains which originate from CH_3 species followed by CH_2 insertion can subsequently be formed out of these initial species. The bond chemically bound to the catalytic active site at the terminal carbon can be broken, thus terminating the chain growth. Generally speaking, two termination pathways are possible, namely thermodynamically favorable β-dehydrogenation to 1-olefins or α-hydrogenation to *n*-paraffins (constant rate ratio of about 70–80%), producing FT primary products rich in 1-olefins [53–56]. Such a chain growth mechanism will obey the ASF polymerization theory that a molar distribution is decreased exponentially with chain length (*n*). The prerequisite for following polymerization theory is that the desorbed C_nH_{2n} or C_nH_{2n+2} from the metal surface does not readsorb onto the catalyst surface for subsequent secondary reactions.

Iron-based catalysts for FTS can give high 1-olefin contents in 60–80% molar ratio independent on residence time because 1-olefin readsorption onto the Fe sites for secondary reactions is poor [57,58]. In the case of Co-based catalysts, 1-olefins are easily readsorbed onto catalytic sites for many competitive reactions such as hydrogenation (Scheme 1, pathway 1) [59–62], dehydrogenation (Scheme 1, pathway 2), reinsertion (Scheme 1, pathway 3) [9,20,21,63], and hydrogenolysis (Scheme 1, pathway 4) [64–71] when they cannot immediately escape from catalyst surface due to diffusion limitations.

Hydrogenation of the 1-olefins into *n*-paraffins in the same carbon number has no direct impact on ASF pattern. In contrast, the hydrogenolysis and the reinsertion will shift the carbon number distribution and result in deviations from Schulz-Flory law [9,20,21,63–71]. The hydrogenolysis of *n*-paraffins and 1-olefins will shorten the chain length to lighter hydrocarbons. On the contrary, 1-olefin reinsertion by CH_2 species can grow the chain length to higher hydrocarbons. Thus, controlling pathway for secondary reactions becomes important for a higher selectivity in desired hydrocarbons.

As mentioned above, wax and middle distillates are favorable products for FTS due to their high grade for direct use. In addition, the wax could be selectively hydrocracked into light hydrocarbons rich in isoalkanes as premium gasoline fuel and diesel fuel, in which the undesired gas products (C_{1-2}) are produced in negligible yields because the carbenium ion mechanism rather than a free radical reaction is always responsible for hydrocracking hydrocarbons with synthetic zeolites [5]. Therefore, an enormous amount of research on FTS aims at selective synthesis of wax and middle distillates [23,72–75].

In general, two approaches can be utilized for controlling selectivity of hydrocarbons in FTS. One is to promote the original chain growth probability (α value) by modifying catalyst structures and components, utilizing reaction phases (supercritical-, gas–liquid–solid-, and slurry- phase), and selecting suitable reaction parameters such as low temperature, low H_2/CO ratio in feed gas. However, the original chain growth mechanism does always yield a Schulz-Flory distribution, which limits selective synthesis of FT products in heavy hydrocarbons. The other way is to initiate the chain propagation (Scheme 1, pathway 3) by *in situ* formed 1-olefins. Chain growth via this approach cannot only convert reactive 1-olefins into heavier hydrocarbons by successive CH_2 incorporation but also suppress the original chain growth [31,32]. Suppressing original chain growth will directly decrease the selectivity of light products.

Although FTS produces high 1-olefin contents, the 1-olefins readsorbed to form alkyl-metal species for secondary reactions are mainly hydrogenated (Scheme 1, pathway 1). The reaction manner is considerably different from the original growing alkyl-metal species (CH_2 insertion as the main pathway) [31,32]. As reported

Table 5
Effect of catalyst on the product selectivity of FTS.

Entry	Catalyst	$P_{after\ reaction}$ (MPa)	CO conversion (%)	Selectivity (%)					
				C_1	C_2	C_{3-4}	C_{5-9}	C_{10-20}	C_{21-40}
1[a]	Co_3O_4	2.9	54.7	5.7	0.9	4.8	20.7	13.8	54.2
2	5 atom% Au/Co_3O_4	1.7	74.5	5.6	1.4	5.7	19.1	13.5	54.7
3	10 atom% Au/Co_3O_4	2.1	68.3	12.3	8.3	22.9	25.7	8.1	22.7
4	25 atom% Au/Co_3O_4	3.2	49.8	11.5	5.9	17.9	27.1	12.3	25.2

Reaction conditions: catalyst = 150 mg; *T* = 230 °C; $P_{initial\ synthesis\ gas}$ = 6 MPa ($Ar/CO/H_2$ = 3/32.3/64.7); reaction time = 11 h; solvent *n*-decane = 14.6 g; water vapor added = 14.6 g; the reactions were carried out in a closed autoclave reactor.

[a] Before run, the catalyst was *in situ* reduced with H_2 1.0 MPa in 20 ml *n*-decane at 350 °C for 2.5 h.

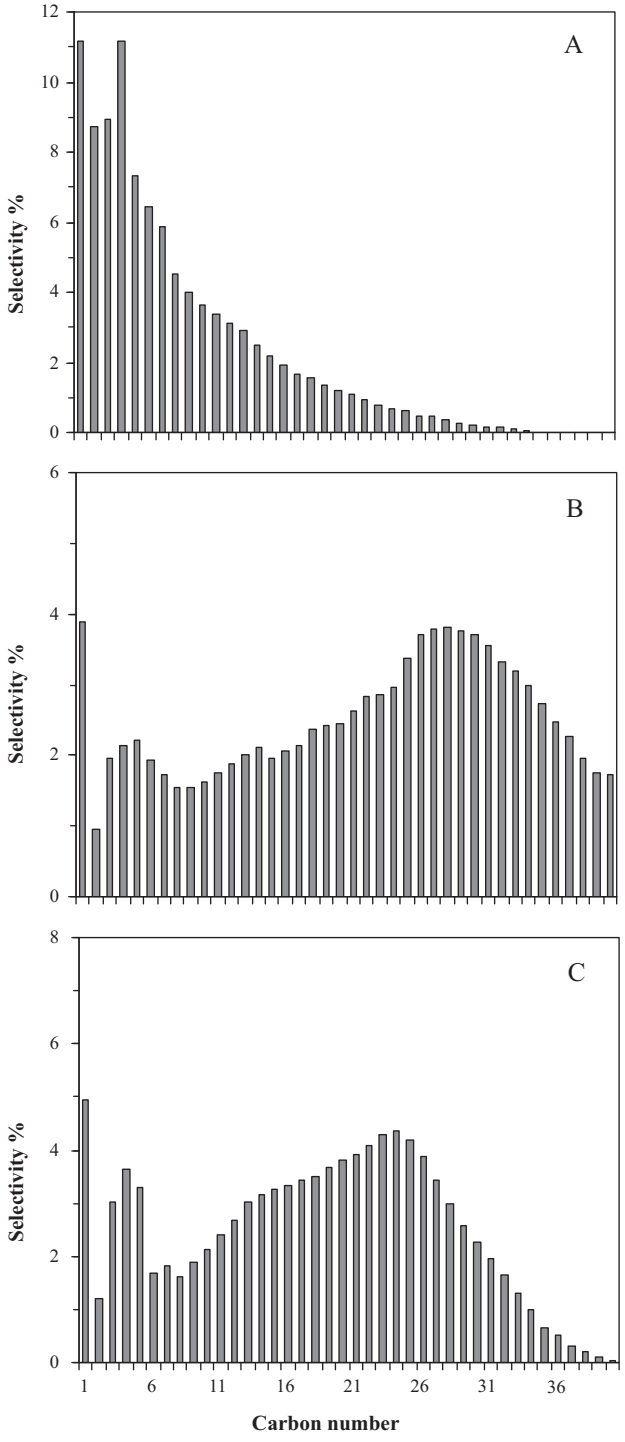

Fig. 4. Effect of water addition on the product selectivity. Reaction conditions: catalyst 150 mg; solvent *n*-decane 14.6 g; T = 230 °C; Pinitial syngas = 6 MPa (Ar/CO/H_2 = 3/32.3/64.7). (A) no addition; (B) 10 mmol water vapor; (C) 10 mmol water liquid.

in previous publications, the large difference in 1-olefin contents in FTS does not obviously change the carbon number distribution and the chain growth probability (α value) [28–30]. Co-feeding 1-olefin experiments also confirm the 1-olefins added are mainly hydrogenated, only small part of the added 1-olefins are utilized as initiator for chain growth, which leads to ineffective utilization [31,32]. Despite anti-ASF pattern obtained in olefin-added FTS, it is not economical because 1-olefins themselves are very useful chemicals.

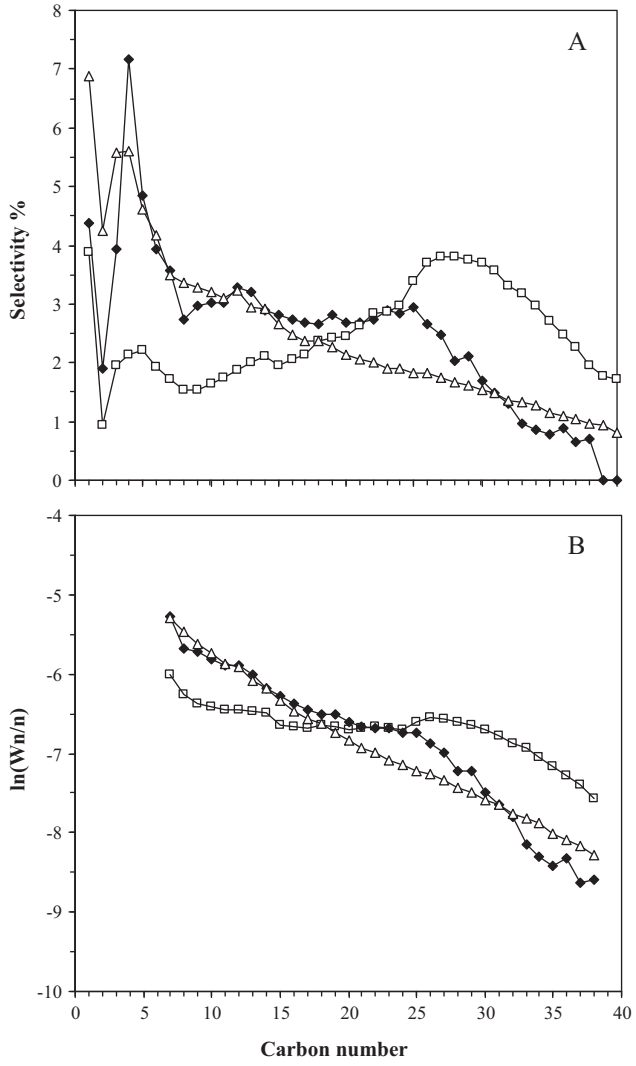

Fig. 5. Effect of time on stream (TOS) on the product selectivity and ASF pattern. Reaction conditions: Co3O4 150 mg; solvent *n*-decane 14.6 g; T = 230 °C; water vapor 10 mmol; $P_{\text{initial syngas}}$ = 6 MPa (Ar/CO/H2 = 3/32.3/64.7). (□) 11 h; (♦) 23 h; (△) 42 h. (A) Hydrocarbon selectivities; (B) product distribution.

Thus, suppressing the 1-olefin hydrogenation into *n*-paraffin while promoting the chain growth become quite difficult target in FTS because Co metal is favorable for hydrogenation reaction. Kinetically, the hydrogenation for adsorbed 1-olefins is always faster than the chain growth by CH_2 insertion.

Water is a primary oxygen-containing product in FTS as oxygen atoms of CO, which is predominantly removed as water on Co-based catalysts. The effects of water on FTS over supported or unsupported Co-based catalysts are studied in both fixed-bed and slurry-phase reactors by several researchers [33–39]. In literature, a remarkable release from ASF pattern has not appeared over various catalysts in the presence of water, although there are lower methane and higher C_{5+} selectivities in some cases [45,76,77]. As shown in our studies (Fig. 4), addition of small amount of water (H_2O/CO = 0.15 molar ratio) in FTS over unsupported Co_3O_4 catalysts in a batch slurry phase reactor could dramatically change the carbon number distribution so that the selectivity of hydrocarbon increases along with an increase in carbon number (n) over a wide range (n = 8–30). The positive effect may be due to increasing surface concentration of active carbon in the presence of water. Bertole et al. has developed a simple 'surface crowding' kinetic model explaining the simultaneous increase in surface concen-

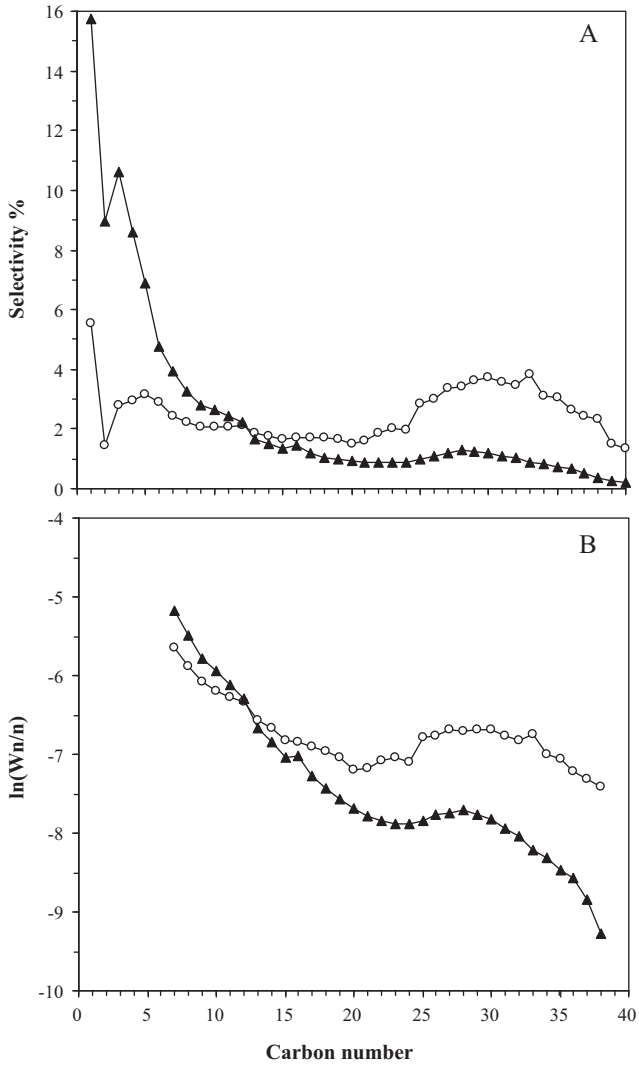

Fig. 6. Effect of reaction temperature on the product selectivity and ASF pattern. Reaction conditions: 5 atom% Au/Co_3O_4 150 mg; solvent *n*-decane 14.6 g; water vapor addition 10 mmol; $T = 230\,^{\circ}C$; Pinitialsyngas = 6 MPa (Ar/CO/H_2 = 3/32.3/64.7). (○) 230 °C; (△) 250 °C. (A) Hydrocarbon selectivities; (B) product distribution.

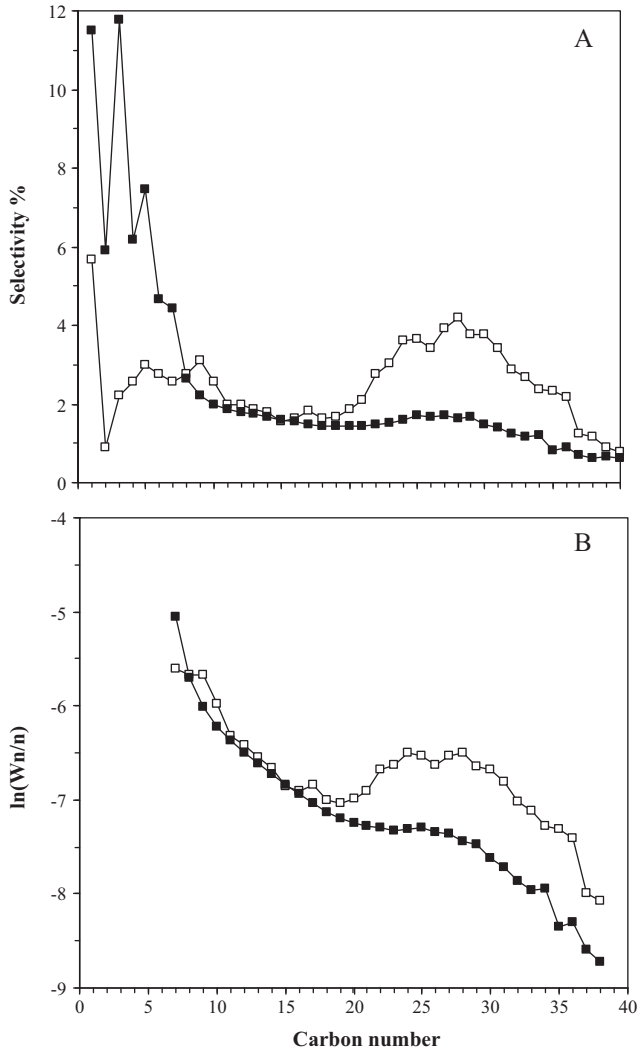

Fig. 7. Effect of gold loading on the product selectivity and ASF pattern. Reaction conditions: catalyst 150 mg; solvent *n*-decane 14.6 g; $T = 230\,^{\circ}C$; water vapor addition 10 mmol; $P_{\text{initial syngas}}$ = 6 MPa (Ar/CO/H_2 = 3/32.3/64.7). (□) Co_3O_4, before run, the catalyst was *in situ* reduced with H_2 1.0 MPa at 350 °C for 2.5 h; (■) 25 atom% Au/Co_3O_4. (A) Hydrocarbon selectivities; (B) product distribution.

tration and decrease in methane selectivity [39]. In our report, a remarkable deviation from ASF pattern could be mainly attributed to chain growth by *in situ* formed 1-olefins.

As it is well confirmed, water can inhibit secondary hydrogenation of 1-olefins [48]. Thus, more 1-olefins are available for chain growth. In other open fixed-bed or slurry phase systems, light 1-olefins can flow out of reactor under reaction conditions, which decreases the residence time for secondary chain growth. In a batch slurry phase reactor, all *in situ* formed 1-olefins can be utilized back and forth going along the route below (also see pathways 2 and 3 in Scheme 1) before they are terminated as *n*-paraffins.

1 – olefin readsorption → chain growth → desorption to 1-olefin

→ readsorption (desorpted 1-olefin) → chain growth—- →

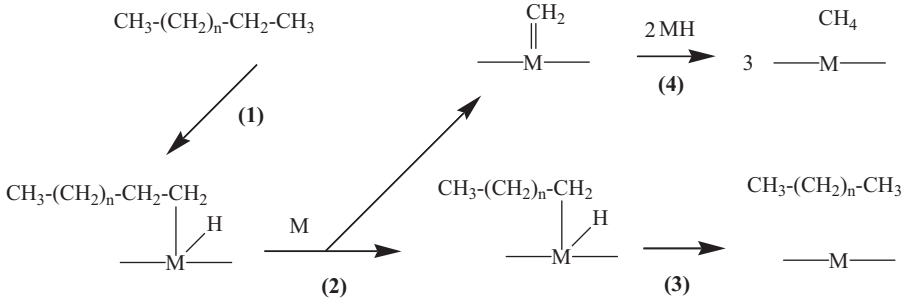

in which M indicates a surface adsorption site

Scheme 2. A possible mechanism for *n*-alkane hydrogenolysis by *α*-scission over Au/Co_3O_4 catalyst.

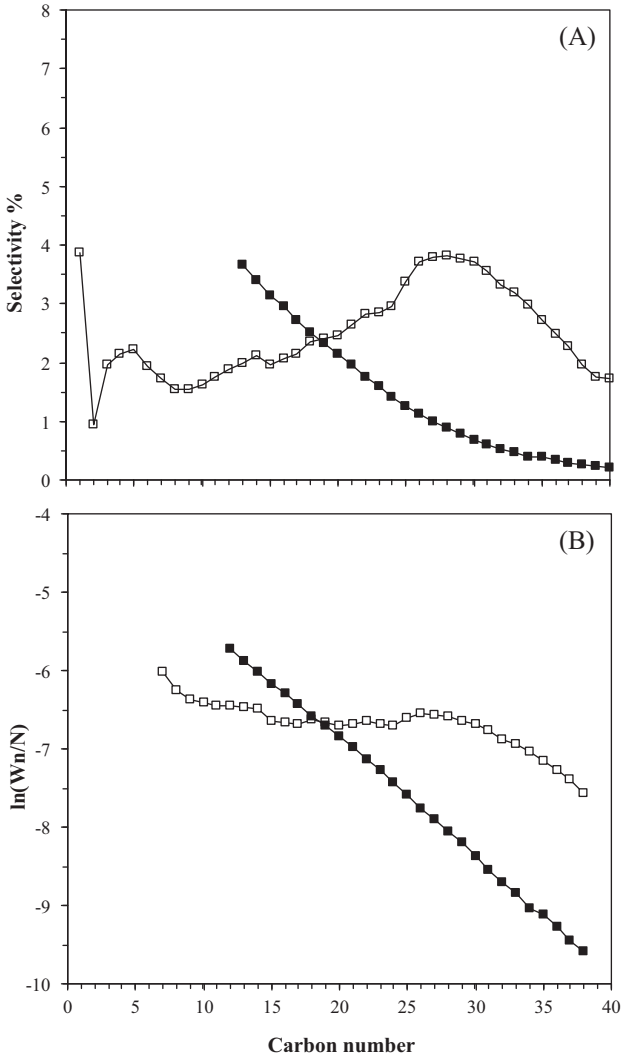

Fig. 8. Effect of H2 treatment of the FT products on the ASF pattern. Reaction conditions: Co_3O_4 150 mg. (□) The case of 23 h in Fig. 5, before treatment; (■) the products were treated with H2 at 230 °C and 3 MPa for 30 h.

In the absence of water, secondary hydrogenation is the main reaction pathway leading to a conventional ASF pattern, although the reaction was carried out in a closed system. By adding water in FTS, water may lower the barriers to CO dissociation due to direct interaction between the weak hydrogen bonding of water and the oxygen of CO. As a result, the surface carbon crowded makes catalyst surface rich in CH_2 species. Thus formed surface poor in H and rich in CH_2 does favor in both original and secondary chain growth. Ratio of secondary chain growth by CH_2 incorporation to chain termination by hydrogenation is notably increased as shown in Scheme 1 (pathways 1 and 3), which is responsible for a remarkable release from ASF pattern. This explanation is in agreement with experimental data. As shown in Figs. 6 and 7A, a high reaction temperature (250 °C) or a high gold loading (10 or 25 atom%) always led to a very high selectivity in light hydrocarbons, although the reaction proceeds in the presence of water. It may be explained that high temperature or high gold loading promotes the rate of supplying atomic H and thus the chain termination to light paraffins is increased. Once *n*-paraffins are formed, secondary chain growth cannot be continued.

Secondary hydrogenolysis also plays an important role in controlling the selectivity of hydrocarbons [64–71]. The hydrogenolysis is strongly dependent upon the reaction conditions. As shown

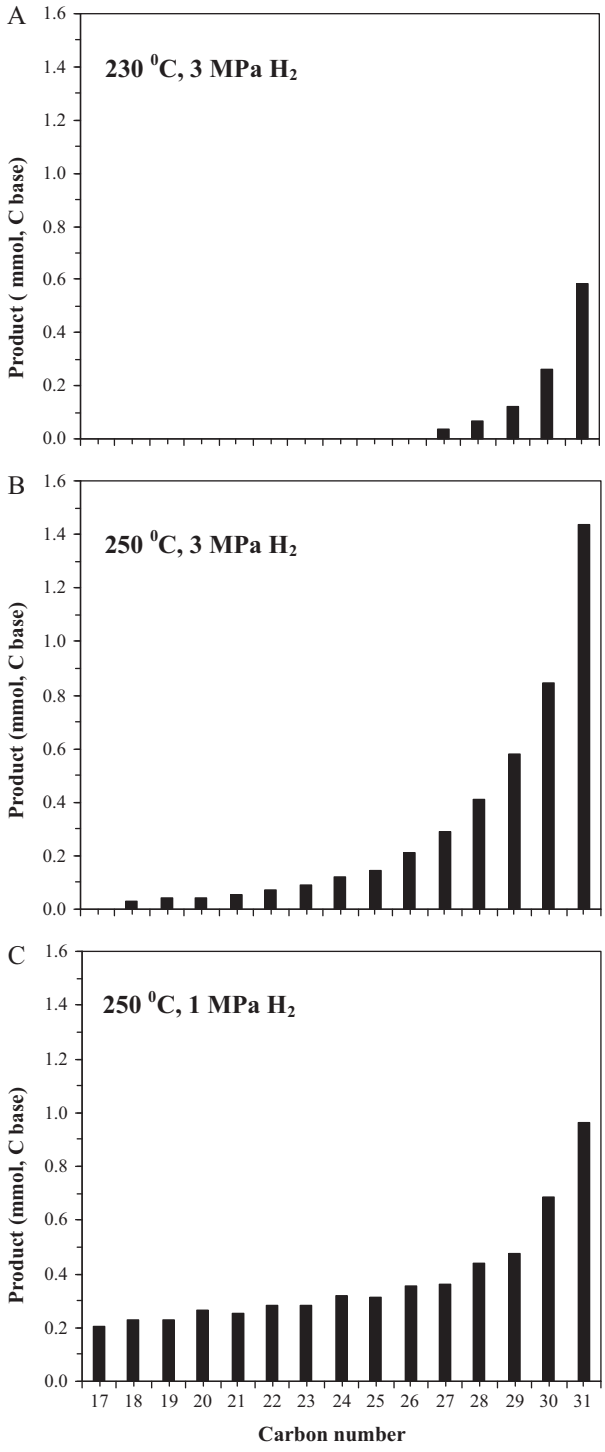

Fig. 9. *n*-Dotriacontane (n-$C_{32}H_{66}$) hydrogenolysis over Co_3O_4 catalyst at different conditions. Reaction conditions: 150 mg Co3O4, solvent *n*-decane = 1028 mmol (C base), *n*-dotriacontane = 42.7 mmol (C base), reaction time = 30 h. Total products (C_{17-31}) and conversion of *n*-dotriacontane for (A) 1.1 mmol and 2.6%; (B) 4.4 mmol and 10.3%; (C) 5.7 mmol and 13.5%.

in Fig. 9, a high temperature and/or a low H_2 partial pressure in the absence of CO can promote the hydrogenolysis rate. A possible mechanism on *n*-alkane hydrogenolysis is described in Scheme 2. C–H bond is activated on Co metal to form *n*-alkyl–Co–H (pathway 1). The *n*-alkyl–Co–H gives shorter *n*-alkyl–Co–H and CH_2=Co by α-scission (pathway 2). The intermediates *n*-alkyl–Co–H and CH_2–Co could be terminated as *n*-alkane (pathway 3) and methane (pathway 4) by hydrogenation. Higher temperatures may be favorable

for C–H bond activation and C–C bond cleavage, which results in higher reaction rates. When the H_2 partial pressure is increased, the hydrogenolysis rate becomes slower. It can be explained that a high H_2 partial pressure may increase the coverage of H on Co metal and the number of catalytic sites for *n*-alkane activation is decreased. A high atomic H concentration on catalytic surface makes the termination of *n*-alkyl–Co–H chains faster and thus inhibits the successive α-scission to lighter hydrocarbons. Since addition of H to 1-olefins forming *n*-alkyl-Co chain is easier than C–H bond activation in *n*-alkane, *n*-alkane hydrogenolysis becomes much more difficult than 1-olefins. In literature, hardly any information can be found on the *n*-alkane hydrogenolysis during FTS, although there are some indications that it can occur [62,65,78]. In addition, the hydrogenolysis reaction can be suppressed by CO because CO poisons C–C, C–H, and H–H bond breaking reactions. In conventional FTS conditions, product hydrogenolysis for both *n*-alkanes and 1-olefins is negligible due to the low reaction temperature and the high CO partial pressure. In contrast, a low CO partial pressure will greatly increase the hydrogenolysis rate. As shown in Fig. 5A, the formed heavy hydrocarbons are converted into light hydrocarbons resulting from the low syngas pressure when the reaction time extends from 23 h to 42 h, which indicates that the chain growth is reversible.

To this end, we can draw key points on how to obtain anti-ASF pattern in a great deviation in FTS catalyzed by Co-based catalysts. First, designed catalysts and reaction parameters lead to a high chain growth factor (α). Second, reactors and process systems selected for FTS facilitate readsorption of reactive 1-olefins and their contact time on catalyst surface as long as possible. Third, secondary reactions for the 1-olefin hydrogenation and hydrogenolysis should be suppressed to promote its initiation to chain growth. By the addition of water, the most challenging control for secondary reaction pathways can be overcome shifting the 1-olefin hydrogenation to its chain growth by CH_2 incorporation.

5. Conclusions

In summary, we have shown that addition of small amount of water to FTS exhibits a remarkable anti-ASF pattern in the carbon number distribution by efficient utilization of *in situ* formed 1-olefins, which is a simple but an economical approach to break the classical ASF pattern for a higher selectivity in more valuable products. The anti-ASF patterns obtained might be mainly attributed to (1) water helping the CO dissociation and thus making a surface crowding of CH_2 but atomic H poor that favors the chain growth of *in situ* formed 1-olefins and suppresses undesired their hydrogenation to *n*-paraffins (2) long residence time for repeated utilization for *in situ* formed 1-olefins especially light 1-olefins in a batch slurry phase reactor. This work provides an example regarding the controlling of the reaction pathways on intermediates towards the production of value-added products. Similar to this example, there may be a wide potential development in maximizing the formation of value-added products by designing or controlling the reaction route towards more efficient synthesis.

Acknowledgments

This work was supported by a Grand-in-Aid for Global COE Program, "Science for Future Molecular Systems" from the Ministry of Education, Culture, Sports, Science and Technology of Japan (2009B1007).

References

[1] (a) F. Fischer, H. Tropsch, Brennstoff-Chem. 7 (97) (1926);
(b) F. Fischer, H. Tropsch, Brennstoff-Chem. 11 (489;) (1930);
(c) E.M. Dry, Catal. Today 71 (2002) 227–241;
(d) H. Schulz, Appl. Catal. 186 (1999) 3–12;
(d) I. Wender, Fuel Process. Technol. 48 (1996) 189–297;
(e) A.A. Adesina, Appl. Catal. A: Gen. 138 (1996) 345–367.
[2] X.H. Li, K. Asami, M.F. Luo, K. Michiki, N. Tsubaki, K. Fujimoto, Catal. Today 84 (2003) 59–65.
[3] Y. Yoneyama, X.Y. Sun, T.Sh. Zhao, T.J. Wang, T. Iwai, K. Ozaki, N. Tsubaki, Catal. Today 149 (2010) 105–110.
[4] X.G. Li, J.J. He, M. Meng, Y. Yoneyama, N. Tsubaki, J. Catal. 265 (2009) 26–34.
[5] X.H. Li, X.H. Liu, Zh.–W. Liu, K. Asami, K. Fujimoto, Catal. Today 106 (2005) 154–160.
[6] J. Bao, J.J. He, Y. Zhang, Y. Yoneyama, Y. Tsubaki, Angew. Chem. Int. Ed. 47 (2007) 353–356.
[7] K.M. Cho, S.Y. Park, J.G. Seo, M.H. Youn, S.–H. Baeck, K.–W. Jun, J.S. Chung, I.K. Song, Appl. Catal. B: Environ. 83 (2008) 195–201.
[8] J.C. Kang, Sh.L. Zhang, Q.H. Zhang, Y. Wang, Angew. Chem. Int. Ed. 48 (2009) 2565–2568.
[9] L. Fan, K. Yoshii, Sh.R. Yan, J.L. Zhou, K. Fujimoto, Catal. Today 36 (1997) 295–304.
[10] Sh.R. Yan, L. Fan, Zh.X. Zhang, J.L. Zhou, K. Fujimoto, Appl. Catal. A: Gen. 171 (1998) 247–254.
[11] G. Henrici-Olivé, S. Olivé, Angew. Chem. Int. Ed. 15 (1976) 136–141.
[12] Ch.–X. Xiao, Zh.P. Cai, T. Wang, Y. Kou, N. Yan, Angew. Chem. Int. Ed. 47 (2008) 746–749.
[13] G.P. Van der Laan, A.A.C.M. Beenackers, Catal. Rev. Sci. Eng. 41 (1999) 255–318.
[14] J.S. Girardon, S.A. Lermontov, L. Gengembre, P.A. Chernavskii, A. Griboval-Constant, A.Y.J. Khodakov, J. Catal. 230 (2005) 339–352.
[15] Q.H. Zhang, J.C. Kang, Y. Wang, Chemcatchem. 2 (2010) 1030–1058.
[16] G.B. Yu, B. Sun, Y. Pei, S.H. Xie, Sh.R. Yan, M.H. Qiao, K.N. Fan, X.X. Zhang, B.N. Zong, J. Am. Chem. Soc. 132 (2010) 935–937.
[17] B.Ch. Shi, B.H. Davis, Appl. Catal. A: Gen. 277 (2004) 61–69.
[18] I. Puskas, R.S. Hurlbut, Catal. Today 84 (2003) 99–109.
[19] Sh.D. Qin, Ch.H. Zhang, J. Xu, B.Sh. Wu, H.W. Xiang, Y.W. Li, J. Mol. Catal. A: Chem. 304 (2009) 128–134.
[20] E. Iglesia, S.C. Reyes, R.J.J. Madon, Catalysis 129 (1991) 238–256.
[21] R.J. Madon, S.C. Reyes, E.J. Iglesia, Phys. Chem. 95 (1991) 7795.
[22] Selectivity control and catalyst design in the Fischer-Tropsch synthesis: sites, pellets, and reactors, in: E. Iglesia, S.C. Reyes, R.J. Madon, S.L. Soled, E.E. Eley, H. Pines, P.B. Weisz (Eds.), Advances in Catalysis, 39, Academic Press, New York, 1993, 221-302.
[23] E. Iglesia, Appl. Catal. A: Gen. 161 (1997) 59–78.
[24] E.W. Kuipers, C. Vinkenburg, I.H. Wilson, H. Oosterbeek, J. Catal. 152 (1995) 137–146.
[25] E.W. Kuipers, C. Scheper, J.H. Wilson, H. Oosterbeek, J. Catal. 158 (1996) 288–300.
[26] L.-M. Tau, A. Dabbagh, B.H. Davis, Energy Fuels 4 (1990) 94–99.
[27] W.H. Zimmerman, D.B. Bukur, S. Ledakowicz, Chem. Eng. Sci. 47 (1992) 2707–2712.
[28] X.H. Liu, W.Sh. Linghu, X.H. Li, K. Asami, K. Fujimoto, Appl. Catal. A: Gen. 303 (2006) 251–257.
[29] K. Yokota, K. Fujimoto, Ind. Eng. Chem. Res. 30 (1991) 95–100.
[30] L. Fan, K. Fujimoto, Appl. Catal. A: Gen. 186 (1999) 343–354.
[31] X.H. Liu, X.H. Li, K. Fujimoto, Catal. Commun. 8 (2007) 1329–1335.
[32] X.H. Liu, X.H. Li, Y. Suehiro, K. Fujimoto, Appl. Catal. A: Gen. 333 (2007) 211–218.
[33] S. Krishnamoorthy, M. Tu, M.P. Ojeda, D. Pinna, E. Iglesia, J. Catal. 211 (2002) 422–433.
[34] A.M. Hilmen, D. Schanke, K.F. Hanssen, A. Holmen, Appl. Catal. A: Gen. 186 (1999) 169–188.
[35] M. Rothaemel, K.F. Hanssen, E.A. Blekkan, D. Schanke, A.M. Hilmen, Catal. Today 38 (1997) 79–84.
[36] G. Jacobs, T.K. Das, P.M. Patterson, J. Li, L. Sanchez, B.H. Davis, Appl. Catal. A: Gen. 247 (2003) 335–343.
[37] G. Jacobs, P.M. Patterson, T.K. Das, M. Luo, B.H. Davis, Appl. Catal. A: Gen. 270 (2004) 65–76.
[38] J. Li, G. Jacobs, T. Das, Y. Zhang, B.H. Davis, Appl. Catal. A: Gen. 236 (2002) 67–76.
[39] C. Bertole, C.A. Mims, G. Kiss, J. Catal. 210 (2002) 84–96.
[40] E. Iglesia, S.L. Soled, R.A. Fiato, G.H. Via, J. Catal. 143 (1993) 345–368.
[41] B. Jager, R. Espinoza, Catal. Today 23 (1995) 17–28.
[42] I. Yates, C.N. Satterfield, Energy Fuels 5 (1991) 168–173.
[43] P.J. Van Berge, J. Van de Loosdrecht, S. Barradas, A.M. Van der Kraan, Catal. Today 58 (2000) 321–324.
[44] C. J. Kim, US Patent 0,355,216 (1993).
[45] M. Claeys, E.V. Steen, Catal. Today 71 (2002) 419–427.
[46] X.H. Liu, B.Sh. Hu, K. Fujimoto, M. Haruta, M. Tokunaga, Appl. Catal. B: Environ. 92 (2009) 411–421.
[47] T. Nowitzki, A.F. Carlsson, O. Martyanov, M. Naschitzki, V. Zielasek, T. Risse, M. Schmal, H.-J. Freund, M. Bäumer, J. Phys. Chem. C 111 (2007) 8566–8572.
[48] T.K. Das, W. Conner, G. Jacobs, J. Li, K. Chaudhari, B.H. Davis, Proceedings of the 7th Natural Gas Conference, Dalian, China, June 6–10, 2004, pp. 331–336.
[49] M.S. Niasari, F. Davar, M. Mazaheri, M. Shaterian, J. Magn. Magn. Mater. 320 (2008) 575–578.
[50] J.L. Gu, W. Fan, A. Shimojima, T. Okubo, J. Solid State Chem. 181 (2008) 957–963.
[51] A.M. Saib, A. Borgna, J. van de Loosdrecht, P.J. van Berge, J.W. Niemantsverdriet, Appl. Catal. A: Gen. 312 (2006) 12–19.
[52] G. Henrici-Olive, S. Olive, in: F.R. Hartley, S. Patai (Eds.), The Chemistry of the Metal-Carbon Bond, 3, Wiley, New York, 1985, Chap. 9.

[53] M. Kaminsky, N. Winograd, G. Geoffroy, M.A. Vannice, J. Am. Chem. Soc. 108 (1986) 1315–1316.
[54] H. Yamasaki, Y. Kobori, S. Naito, T. Onishi, K. Tamaru, J. Chem. Soc. Faraday Trans. 77 (1981) 2913.
[55] W. Erley, P. McBreen, H. Ibach, J. Catal. 84 (1983) 229–234.
[56] C.J. Wang, J.G. Ekerdt, J. Catal. 86 (1984) 239–244.
[57] H. Schulz, H. Gökcebay, in: J.R. Kosak (Ed.), Catalysis of Organic Reactions, Marcel Dekker, New York, 1984, p. 153.
[58] H. Hayakawa, H. Tanaka, K. Fujimoto, Appl. Catal. A: Gen. 328 (2007) 117–123.
[59] S. Novak, R.J. Madon, H. Suhl, J. Catal. 77 (1982) 141–151.
[60] S.Z. Roginsky, Preceedings, 3rd International Congress on Catalysis, Amsterdam, 1964; Wiley: New York, 1965, p. 939.
[61] W.K. Hall, R.J. Kokes, P.H. Emmett, J. Am. Chem. Soc. 82 (1960) 1027–1037.
[62] H. Schulz, B.R. Rao, Elstner, M. Erdoel Kohle 23 (1970) 651.
[63] K. Fujimoto, Top. Catal. 2 (1995) 259–266.
[64] K.R. Krishna, A.T. Bell, Catal. Lett. 14 (1992) 305–313.
[65] H. Pichler, H. Schulz, Chem. Ing. Tech. 42 (1970) 1162–1174.
[66] Y.T. Eidus, Russ. Chem. Rev. 36 (1967) 338.
[67] W. Molina, V. Perrichon, R.P.A. Sneeden, P. Turlier, Catal. Lett. 13 (1980) 69.
[68] R. Snel, R.L. Espinoza, J. Mol. Catal. 54 (1989) 103–117.
[69] R. Snel, R.L. Espinoza, C1 Mol. Chem. 1 (1986) 349.
[70] L.T. Percy, R.I. Walter, J. Catal. 121 (1990) 228–235.
[71] E. Gibson, J. Chem. Ind. 21 (1957) 649.
[72] N. Tsubaki, K. Yoshii, K. Fujimoto, J. Catal. 207 (2002) 371–375.
[73] D. Pinna, E. Tronconi, L. Lietti, L.R. Zennaro, P. Forzatti, J. Catal. 214 (2003) 251–260.
[74] J. Panpranot, S. Kaewkun, P. Praserthdam, J.G. Goodwin Jr., Catal. Lett. 91 (2003) 95–102.
[75] J. Van de Loosdrecht, M. Van der Haar, A.M. Van der Kraan, A.J. Van dillen, J.W. Geus, Appl. Catal. A: Gen. 150 (1997) 365–376.
[76] A.K. Dalai, T.K. Das, K.V. Chaudhari, G. Jacobs, B.H. Davis, Appl. Catal. A: Gen. 289 (2005) 135–142.
[77] S. Storsæter, Ø. Borg, E.A. Blekkan, A. Holmen, J. Catal. 231 (2005) 405–419.
[78] C.S. Kellner, A.T. Bell, J. Catal. 70 (1981) 418–432.